Annu. Rev. Phys. Chem. 2000. 51:601–22

SELF-ASSEMBLED CERAMICS PRODUCED BY COMPLEX-FLUID TEMPLATION

Daniel M. Dabbs and Ilhan A. Aksay
Department of Chemical Engineering and Princeton Materials Institute, Princeton University, Princeton, New Jersey 08544; e-mail: iaksay@princeton.edu

Key Words amphiphiles, biomimetics, self-assembly

■ **Abstract** This review examines the use of self-assembly in the fabrication of ceramic mesostructures, emphasizing the use of amphiphilic surfactants and block copolymers. The association between this area of research and biomimetics is discussed, linking developments in synthetic self-assembly with biomineralization. The fabrication of hierarchical structures through the use of simultaneous processing is shown to be a necessary condition for applications of this new technology.

INTRODUCTION

We review recent progress in the synthesis and processing of nanostructured ceramics through self-assembly, emphasizing the use of complex fluids as structure-directing agents. The ceramic materials are produced by the templation of complex-fluid systems that define unique structures (within the length scale of 1–100 nm) through self-assembly (1; Figure 1). These complex fluids, which are based on amphiphilic building blocks (Figure 2) or colloidal particles, can produce well-defined nanostructures (also referred to as mesogenic materials) at a scale of <100 nm, owing to two factors: (*a*) the size of the building blocks and (*b*) the weak interactions between the building blocks, which allow easy manipulation of the structures at low temperatures ($<100^{\circ}$C). Here we emphasize the use of amphiphilic polymers, and we refer the interested reader to the burgeoning literature on the use of colloidal patterning in the fabrication of mesostructured materials (e.g. see 2–12).

In contrast to the weak interactions that determine the morphologies of the amphiphiles, ceramic materials, which are constructed with strong ionic or covalent bonds, cannot directly form the types of structures that are displayed by complex fluids. Because of the strong nature of their chemical bonds, their small ($\sim$1-nm) unit cells (building blocks) and the aggregates of these unit cells (grains) produce high-modulus structures. High temperatures ($>0.5\,T_{\mathrm{m}}$, the melting temperature of the material) are needed to impart sufficient atomic (ionic) mobility for the

0066-426X/00/1001-0601$14.00

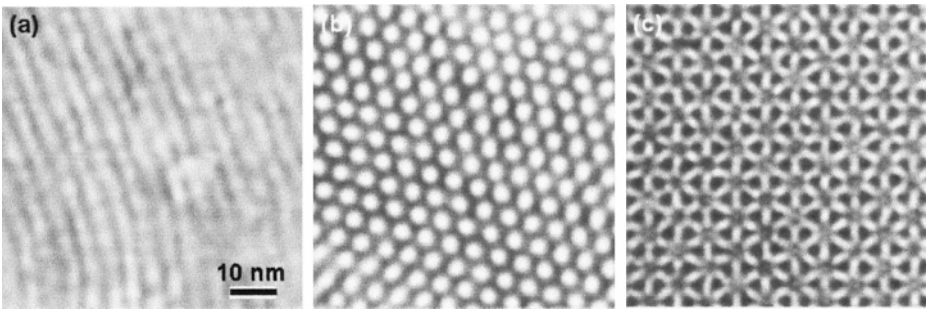

Figure 1 Silica mesostructure from templating (*a*) lamellar, (*b*) hexagonal, and (*c*) cubic liquid–crystalline phases formed by organic surfactants in solution (1). The scale bar is the same for all three images (1, 15).

modulation of the structural features. At such high temperatures, it is difficult to retain any deliberately introduced nanostructural features, owing to coarsening.

With the use of inorganic precursors, it is possible to replicate the structures of the complex fluids into a hybrid material [e.g. an organic/inorganic nanostructured composite (13, 14)]. If necessary, the complex fluid portion can be removed later through solvent extraction or pyrolysis, converting the system to a 100% ceramic while retaining the nanostructural features of the complex fluid (1, 13–15; Figure 1). The results of following this pathway are termed self-assembled ceramics, although the self-assembly process itself originates with the complex fluid and not with the ceramic. However, the inorganic precursors may play an active role in the process, effecting self-assembly within the system.

Self-assembly of ceramics is a relatively new paradigm in the synthesis and processing of synthetic materials. In the world of biology, however, this is the only approach, and thus it is not a new concept when we discuss biogenic materials (16, 17). A brief survey of biological influences is a more general discussion of

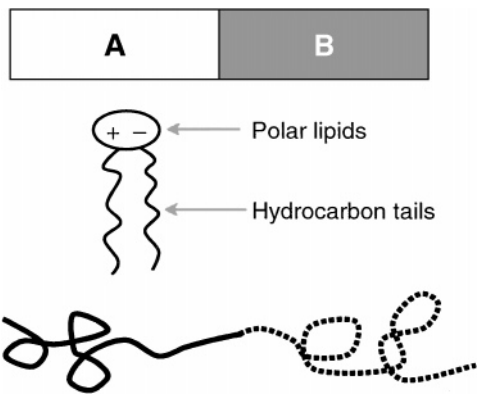

Figure 2 A generalized amphiphile, composed of immiscible components. (*A, B*) Common examples of amphiphilic molecules are surfactants, including detergents, soaps, and biomembrane lipids (*middle*); and block copolymers (*bottom*), such as block copolymer blends of polystyrene (*bottom*, solid line) and polyisoprene (*bottom*, dashed line).

synthetic analogs to the natural processes, describing the myriad supramolecular chemistries that have been and are being used to form nanostructured materials. The biological processes that create the mineralized tissues (e.g. bone, teeth, and shell) have inspired the directed synthesis of ceramic materials through the use of organic molecules (16–21). Long before the study of the natural processes achieved an intellectual critical mass, however, the use of inorganic/organic mixtures—forming ceramic structures from clays—had become commonplace. The technology of the traditional craft of ceramic processing is markedly different in length scale, chemistry, and processing conditions from the corresponding processes observed for natural materials, and until recently there appeared little to connect the synthetic to the natural.

The field of biomimetics is based on the supposition that nature can provide models for processing at the submicrometer scale. Despite the intense interest in the formation of natural materials, current research has moved beyond the restrictions imposed by nature, emphasizing the bioinspired rather than the biomimicked. Many research groups, including our own, seek to exploit supramolecular chemistries to build mesogenic structures at the nanometer scale that resemble biogenic materials in form but use substances and structures that take us beyond nature into purely synthetic functional materials that are designed for specific applications (22–29).

The large number of papers that have appeared within the past 10 years and the many reviews on this topic that reflect the vantage points of different research groups (22–29) make it unnecessary to cite each and every paper. The scope of this review is therefore limited to the application of amphiphilic surfactant solutions and block copolymers (Figures 2 and 3) to the formation of self-assembled ceramics (Figure 1); the general developments in this field are reviewed, and recent work is described that provides examples of these developments. Silica and silicate-based materials dominate this discussion, but this should not be construed as an inherent limitation to the described methodologies. Although silica-based ceramics are the most highly developed materials in this area of study, other ceramic systems have been and are being studied, as noted in the following sections.

BIOMATERIALS AND BIOINSPIRED PROCESSING

Bioinspired processing seeks to adapt lessons from biology in the creation of synthetic analog composites with a unique spectrum of properties (16, 17). It is worth asking whether biomaterials and bioinspired processing should be considered a field of research (19). When we begin by examining the term “biomaterial” itself and the meaning it holds for different researchers within different circumstances, the presence of a synthetic material in a biological environment is insufficient in itself as a suitable definition for a biomaterial (19). In addition, the study of specific processes within a living system, for example, the study of the crystal formation processes in a shell or bone, cannot be included in a broader definition of the term

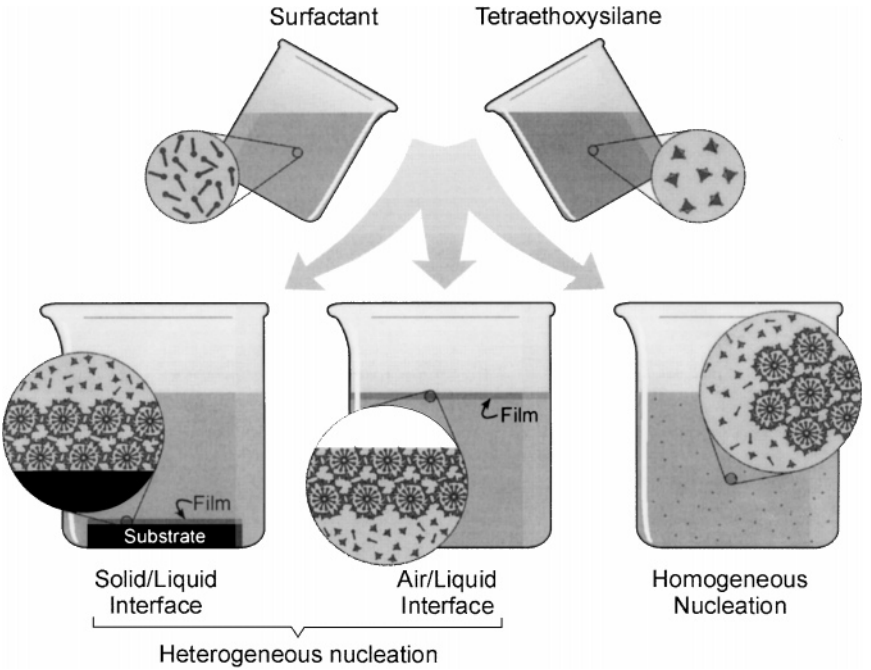

Figure 3 Simple schematics for the fabrication of ordered mesostructures (neither templating nor coassembly is implicit in this drawing). The surfactant or surfactant/inorganic pair spontaneously forms the appropriate micellar structure. In the former situation (templating), the anions will then condense on the hydrophilic surfaces of the micelle. In heterogeneous nucleation, the alignment and structure of the micelles can be influenced by the choice of substrate (*bottom left*) or can occur at the air/water interface (*bottom middle*). (Any nucleation that might occur on the walls of the container is ignored.) In homogenous nucleation, the micelles spontaneously form within the liquid medium (*bottom right*) and aggregate to form mesostructured particles. These may condense to form larger bodies and precipitate from suspension.

if the focus of the study emphasizes the biological process and not its materials aspects (19).

Biomaterials can be defined by turning to the concept of "bioinspiration"—that is, the extent to which the development of a materials system is inspired by biological processes and the ultimate use of the resulting materials. The products of bioinspired research, when used in biomedical applications, provide the most suitable examples of (synthetic) biomaterials. On the other hand, the study of biological materials, pursued in the interests of expanding the field of materials research, retains its importance for further progress in this field. In such cases the research serves as the source of inspiration, encouraging new ideas and approaches to the fabrication of new materials (16, 17, 19). This definition is shared throughout

the materials science community (e.g. see 30, 31) and is based on concepts explored early in the twentieth century (32). In the formation of ceramic materials, we can now move beyond the definition of biomaterials and approach a more generalized application of inorganic/organic interactions in forming mesogenic materials while continuing to acknowledge the natural inspiration.

Biology as a Guide for Materials Synthesis and Processing

In general, natural processes involving the nucleation and growth of inorganic crystals use organic surfaces as templates (20, 33). Understanding this phenomenon remains a principal goal in the area of bioinspired research, but, although research is ongoing and far from achieving a complete understanding, three key features of biological systems have been recognized that provide guidelines for bioinspired research (19–21, 34–36) and for research into the more general question of inorganic/organic interactions.

First, the structures of biological composites are hierarchically organized in discrete levels or scales beginning at the nanometer length scale (37). Virtually all biocomposite systems have at least one distinct structural feature that lies within each length scale and is defined by the molecular, nanoscopic, microscopic, and macroscopic regions. Biogenic "hard" materials are formed in nature through the growth of hierarchically structured organic/inorganic composites. The organic "soft" materials (e.g. proteins, membranes, and fibers) are organized on length scales between 1 and 100 nm and provide the frameworks for the growth of specifically oriented and shaped inorganic compounds (e.g. $CaCO_3$, SiO_2, Fe_3O_4, and hydroxyapatite) with small unit cells ($\sim$1 nm) (16, 17, 20, 34, 38–41). These self-assembled structures provide the nanoscale building blocks for the construction of even larger structures, again through processes involving self-assembly. Because many material properties (such as fracture) do not scale linearly with size, this organization of structures at the nanometer scale yields material properties that are quite different from those predicted by simple rules-of-mixing models (42).

The second guideline from nature involves the assembly and templating processes used in nature to design nanocomposites with desired interfaces and structures within biomaterials. Levels of structural organization are held together by specific interactions between the components. The super-organization of the different components and levels into a hierarchical composite system is controlled by the parent organism's need for structures that satisfy a broad range of functional requirements (43). However, as composite systems increase in complexity, they function at higher levels of performance, which finally results in materials systems that are composed of "intelligent" and/or "adaptive" composites. And although past work has demonstrated that physical properties can be maximized by hierarchical designs (44), the optimization of physical properties through hierarchical design has not yet been tested in products. Research involving hierarchical structures is hampered by the inability to fabricate structures at the nanoscale level, although work is proceeding in promising directions in this area (17–19, 25).

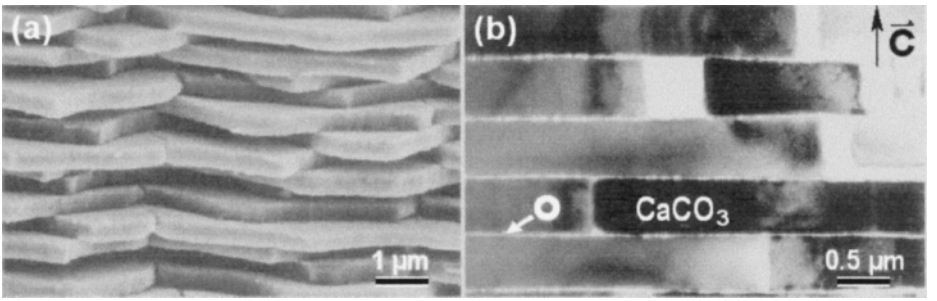

Figure 4 (*a*) Scanning electron microscopy image of fracture surface of aragonite portion of abalone nacre, showing aragonite ($CaCO_3$) platelets ~0.5 μm thick; (*b*) transmission electron microscopy image of the nacre cross-section, revealing a <10-nm-thin organic film (marked O) between aragonite platelets with *c*-axes normal to the organic template. (Reprinted with permission from Reference 18.)

The third guideline taken from nature is the role of specific interactions at the interfaces. In a favored example, an abalone shell consists of layered platelets of $CaCO_3$ (~200 nm thick) that are held together by much thinner (<10 nm) organic polymer "mortar" (18, 45; Figure 4). The organic mortar not only binds the platelets together but also acts as a template to induce the growth of these epitaxially oriented, chemically distinct components (46–48). In this deceptively simple system, the organic component both provides enhanced mechanical properties within the composite structure and serves as the directing agent for the controlled nucleation and growth of the inorganic component, the latter achieved by a mechanism that has not yet been fully determined.

From the standpoint of synthetic processes, it has been shown that laminated hierarchical structures of biogenic systems (e.g. the nacre of abalone shell) can be mimicked in simple synthetic composites built by microlaminating to form ceramic-metal (49–51), ceramic-organic (52), and organic-organic composites. Significant improvements in mechanical properties are observed in the resulting composites. For example, layering B_4C/Al (or SiC/Al or B_4C/polypropylene) composites resulted in significant increases in the mechanical properties (49, 53, 54; Figure 5, see color insert). B_4C/Al composites are strengthened as a result of residual stresses with nanoscale modulations in the interpenetrating network of the ceramic and the metal phases (55). The processing of these ceramic-metal and ceramic-organic microlaminates is based on the concept of infiltrating laminated scaffolding (ceramic) with liquid (metal or organic polymer). The laminated composites thus produced appear structurally similar to nacre but are limited to the micrometer scale owing to the intrinsic limitation of the tape-casting method used (49, 53). To achieve the single most important aspect of structural organization in biogenic systems, processes must be developed to fabricate hierarchical systems with deliberately introduced designs ranging from nanometer to macroscopic dimensions.

At the nanometer length scale, bioinspired processing provides the necessary approach for the design and fabrication of nanostructured organic-inorganic composites through (partial) mimicking of processes, structures, and properties of biogenic hard materials such as shells. Shells, bones, and teeth are of interest to the materials scientist because each of these materials is simultaneously hard, strong, and tough, with unique hierarchical structural features originating at the nanometer scale (16, 17, 20, 56; Figure 6). The emphasis remains the development of enabling science to permit the fabrication of structures with greater similarity to biogenic materials, through the application of self-assembly at the nanometer scale (Figure 7) coupled with lamination and patterning methods at the microscopic scale. The potential of this approach has been exemplified in recent publications (27, 57–74).

In general then, biogenic systems achieve design at the nanoscale through the self-assembly of organic structures. The inorganic structures then form via directed or template-assisted self-assembly, during which the self-assembled organic materials (e.g. proteins and/or lipids) first build the scaffolding that directs the deposition of the inorganic compounds (17, 45). In some cases, structurally organized organic surfaces catalytically or epitaxially induce growth of specifically oriented inorganic thin films (75–77). In addition, natural mineralization involves environmentally balanced, aqueous-solution chemistries at temperatures of $<100^{\circ}$C, giving impetus to research into environmentally benign processing of ceramic composites (78).

NANOSTRUCTURED CERAMICS THROUGH SELF-ASSEMBLY

Mesogenic materials were virtually unknown in ceramic materials (leaving aside zeolites, with characteristic pore diameters of <3 nm) until the discovery that self-assembly could be used to control their nanostructural design (13, 14). Although the first synthetic mesogenic materials were described in the literature as early as 1990 (79), there was little recognition of the significance of this work until researchers at Mobil Research described the synthesis of mesogenic materials under subcritical, hydrothermal, alkaline-processing conditions (13). The Mobil work was preceded by a 1971 patent (80) on the formation of a low-bulk-density silica for catalytic applications, using a method very similar to that developed by Mobil (81, 82), but this earlier work was overlooked for nearly 30 years. Despite this earlier research, the Mobil studies must be credited as sparking the tremendous interest in mesogenic materials during the last decade. A direct consequence of the Mobil researchers' discovery was the rapid development of related processes that prepared mesoscopic particles under acidic conditions (83, 84) at lower temperatures by using less surfactant and requiring less processing time.

For amphiphilic surfactants and polymers (Figure 2), it is usually sufficient to focus on the amphiphile as the "carrier" and the inorganic ion as the "passenger" in

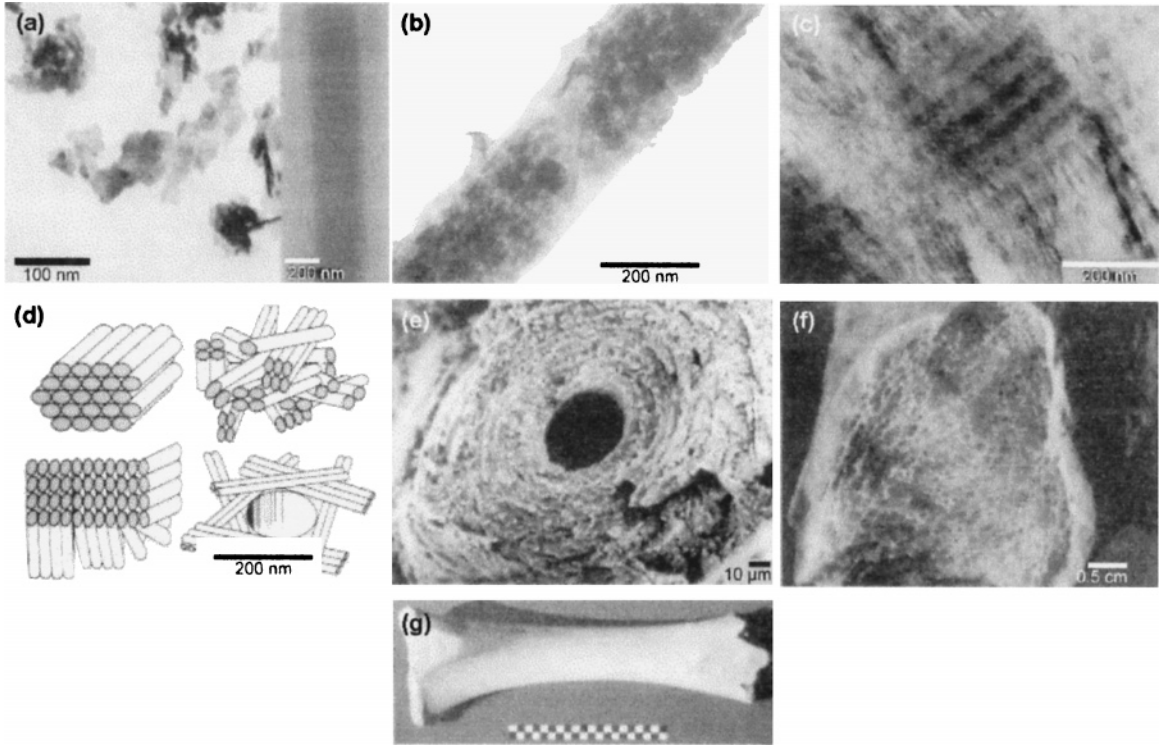

Figure 6 The hierarchical levels of organization within bone. (*a*) Level 1, crystals form human bone (*left*) and part of an unmineralized collagen fibril from turkey tendon (*right*); (*b*) level 2, mineralized collagen fibril from turkey tendon; (*c*) level 3, thin section of mineralized turkey tendon showing fibril array; (*d*) level 4, fibril array patterns of organization found in bone; (*e*) level 5, single osteon from human bone; (*f*) level 6, fractured section from a fossilized human femur; (*g*) level 7, whole bovine bone (scale, 10 cm). (Reprinted with permission from Reference 170.)

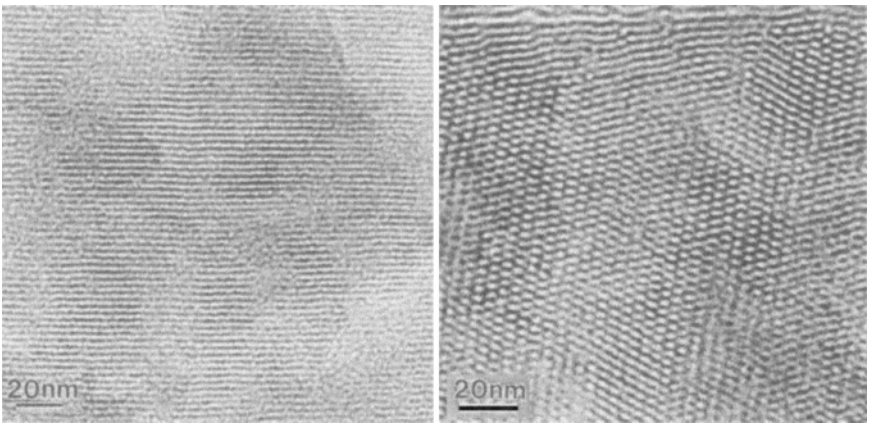

Figure 7 Lateral (*left*) and transverse (*right*) cross-sections of a mesostructured silica film formed on a mica substrate. The channels appear continuous in the view along their length (*left*), while remaining ordered. The anisotropy apparent in the transverse image (*right*) is most probably caused by preferential shrinkage in the direction normal to the surface of the mica substrate during drying. (Reprinted with permission from Reference 18.)

the formation of mesogenic materials. Indeed, the use of a simple templating model was sufficient to produce successful replications of several different mesoporous morphologies soon after the Mobil reports appeared (1, 13–15, 83), with each of the subsequent structures based on a specific surfactant-water mesophase. In this section we limit our discussion to two general classes of amphiphiles: surfactants and block copolymers (Figures 2 and 3) as used in the fabrication of ceramics.

Surfactant-Based Processing

Two general mechanisms for the synthesis of mesoscopic silicates were hypothesized by the Mobil researchers. Either ordering occurs through the simple templating of silica precursor ions onto organic surfactant structures to form solid inorganic replicas of the underlying liquid crystal morphologies, or restructuring occurs through a true coassembly process, which involves the cooperative assembly of the surfactant–inorganic-ion pair into the liquid crystalline structure (13–15; Figure 1). The latter mechanism is indirectly supported in the Mobil work by the observation that the formation of the original hexagonal structures occurs at surfactant concentrations below the critical micelle concentration for the surfactant. So the second model for mesogenic formation uses the surfactant-inorganic pairing itself as the structure-directing entity (83, 85), whereas the first model relies primarily (if not entirely) on the surfactant as the structure determinant. As noted, the utility of the templating model is shown by the rapid development of many different mesostructures within a short span of time after the original Mobil study (1, 13–15, 83–85).

The substantial increase in research on mesostructured ceramics formed by using surfactants as the structure-directing agent is demonstrated by the large body of work focusing on this class of materials (1, 13–15, 18, 58–60, 79–114). Descriptions exist in current literature on the formation of mesogenic particles (58, 59, 84, 86, 90–98), fibers (91, 93, 97), and thin films (18, 60, 67, 99–108) with pore sizes within the range of 5–30 nm (85, 86). Interest in the structure of the pore network is necessarily concomitant with the formation of the different structures. Principal morphologies in ordered surfactant-based systems are the hexagonal (1, 15, 91, 92, 115), cubic (1, 15, 85, 116), and lamellar (86, 90) (Figure 1).

Although most of the cited literature deals with the hexagonal, cubic, and lamellar morphologies, liquid crystals are not limited simply to these ordered micellar or tubular structures. Other three-dimensional morphologies exist in addition to the crystalline structures [with a repeating unit cell such as the cubic and gyroid structures (85, 90, 117, 118)]. These "disordered" structures contain randomized but continuous pore structures whose synthesis relies on electrostatic interactions (58, 59, 119), hydrogen bonding (120–123), and weak van der Waals interactions (124, 125). The disordered bicontinuous morphologies include materials identified as "disordered" (124, 125), "worm-like" (123, 126), and "L_3" structures (58, 59; Figure 8, see color insert), referring to the method of synthesis. The disordered systems provide a path for circumventing a significant disadvantage in the formation of the crystalline structures: the formation of grain boundaries in large structures. The lack of grain boundaries encourages application of disordered materials to the fabrication of monoliths and larger-scale structures (59, 123, 126) as discussed further below.

The general mechanism of formation for these different morphologies, ordered and disordered, depends on the presence of the structure-directing agent *S*—the surfactant—and the inorganic precursor *I*, which interacts with the surfactant to form the mesostructure (84, 86). The nature of the interaction between the inorganic moiety and the organic surfactant determines the mode of synthesis and the morphology of the final material. The "generalized liquid-crystal templating mechanism" (84, 86) can be used to describe (*a*) electrostatic interactions of the type I^--S^+, I^+-S^-, I^+-X^--S^+, I^--M^+-S^-, where M^+ is a metal ion and X^- is a counterion; (*b*) hydrogen bonding involving neutral species, I^0-S^0, I^0-N^0, where N is polyethylene oxide; and (*c*) covalent bonding, S-I. This model serves as a useful guide to the formation of ceramic mesophases from surfactant templation. It can also be extended to include general amphiphiles, such as block copolymers.

After templating, the inorganic precursor condenses to form a rigid cast of the underlying liquid crystal, and the organic phase can be removed to form an inorganic cellular solid composed of a periodic nanoporous structure of uniform diameter and distribution. The resulting materials are locally amorphous at the atomic scale but exhibit crystallinity at longer length scales, that is, tens to hundreds of angstroms. These porous structures may be retained as cellular solids or subsequently reinfiltrated with secondary phases. The controlled pore structure allows for the fabrication of unique composite systems, including oriented nanowires

(127), sensor/actuator arrays (128, 129), catalysts and functionalized membranes (29), and optoelectronic devices (12).

Block Copolymers

Recent developments have revealed another method for the preparation of mesostructured silicate—and by extension other mesoporous ceramics—through the use of block copolymers as structure-directing agents. The processing of ceramics with block copolymers is similar to that of surfactant molecules at a longer length scale, because templating is done on polymers, not surfactants. In these systems, length scales approach those found for the process of biomineralization. Different morphologies can be obtained through the cooperative self-assembly of organic and inorganic moieties across length scales, just as in natural systems. Block copolymers have been used to develop nanostructured organic/organic composites (e.g. see 130) and ceramic/organic composites (67, 131–133), taking advantage of the wide range of morphologies that exist within block copolymer systems (134, 135). These approaches have been used to synthesize, for example, mesoporous materials with large pore sizes (133) and layered structures with a periodic length scale of $\sim$60 nm (136). Amphiphilic triblock copolymers have been used to direct the organization of polymerizing silica species, resulting in hexagonal mesoporous silica structures with uniform pore sizes up to $\sim$300 Å (92). These "SBA-15" materials are synthesized under acidic conditions and are subsequently calcined to yield mesoporous structures. An approach that is more obviously biomimetic uses synthetic cysteine-lysine block "copolypeptides" that mimic the properties of silicatein, a protein found to direct silica growth in certain sponges (137). The synthetic analog hydrolyzes tetraethoxysilane while simultaneously determining the morphology of the silica mesostructure; spheres and columns of amorphous silica are produced by using the reduced and the oxidized forms of the copolymer, respectively (137).

Commercially available block copolymer systems were shown to pattern metal atoms through preferential interactions between the precursor metal ions and Kraton (Shell Chemical Co., Houston, TX) (138, 139), a polystyrene-polybutadiene-polystyrene triblock copolymer. In this material, the thickness of the polymer template can be controlled through spin casting and reactive ion etching (140), and the orientation of the segregated "nanodomains," composed of the different polymer blocks, can be aligned by an electric field (141) and/or the substrate surface (142). A potential application of this technology uses the Kraton as a template for fabricating high-dielectric-constant organic/$BaTiO_3$ nanocomposites.

$BaTiO_3$ is used extensively in multilayer capacitors, thermistors, and electro-optic devices (143, 144) because of its high dielectric constant (1000) (145). It can be synthesized at low temperatures ($<100^{\circ}$C), enhancing its compatibility with processing organic polymers (146, 147). The ceramic has a low breakdown voltage, whereas organic polymers have high breakdown voltages, suggesting that the coupling of barium titanate with an organic polymer should yield a composite with

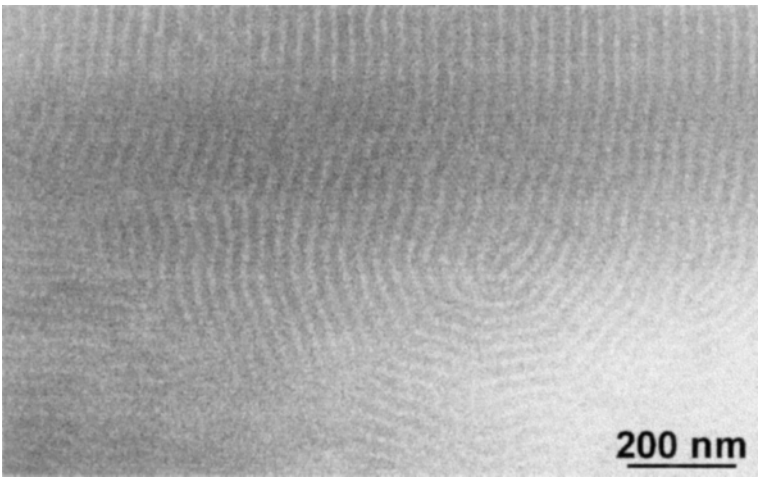

Figure 9 Transmission electron micrograph image of a selectively ceramic-templated block copolymer film (Kraton). This terraced region of the Kraton film contains cylindrical domains of polystyrene (light bands) with interdomain spacing equal to 10 nm, alternating with barium titanated regions (dark bands), which have interdomain spacing of 23 nm. (Reprinted with permission from Reference 148.)

measurably higher breakdown voltage. Nanosized $BaTiO_3$ particles can be formed in situ within Kraton (147, 148). The copolymer self-assembles to yield cylindrical polystyrene nanodomains in a polybutadiene matrix. Amorphous $BaTiO_3$ is grown onto the polybutadiene interdomains (149; Figure 9), whereas the structure of Kraton is preserved throughout the process.

SIMULTANEOUS PROCESSING AT MULTIPLE LENGTH SCALES

The use of amphiphiles to synthesize structures at length scales of <100 nm is now well developed, as shown above. However, it is necessary to translate these building blocks into larger hierarchical systems, which requires retention of the building-block structure during larger-scale assembly. Potential applications for the mesogenic materials will not be realized in the absence of large-scale structures, which have not yet been fabricated. This lack of visible practical applications may threaten further support for and interest in research on the formation of mesostructures. A necessary condition for eventual commercial application requires the formation of controlled shapes and structures in the form of continuous thin films, fibers, and monoliths, with sizes beyond the microscopic particles heretofore synthesized

(18, 104, 105, 150). This section reviews efforts to apply the science of materials self-assembly to the practical synthesis of new material systems, emphasizing fabricating structures at larger length scales (Figures 9 and 10).

Continuous Thin Films

Solid/Liquid Interfaces The supramolecular assembly of surfactant/silicate mesophases to form structured thin films has been studied at solid/liquid interfaces (18, 60, 104–106, 151–153) and at air/liquid interfaces (see the next section). Work has shown that continuous mesoporous silicate films can be grown at the solid/liquid interface of many different substrates. The structure of the first layer of adsorbed surfactant is determined by the effect of the substrate on the surfactant adsorption (18, 60, 86). Previous studies (154, 155) reported that three-dimensional surfactant structures such as cylindrical tubules and spheres can form at solid/liquid interfaces, including hemimicellar structures on poorly orienting amorphous substrates, such as silica, and highly aligned tubular structures on more strongly orienting crystalline substrates, such as mica and graphite (Figure 10, see color insert). The ordered surfaces of mica and graphite can orient adsorbed surfactants through weak anisotropic (van der Waals or electrostatic) attractions between the crystalline substrate and the surfactant molecules. On the other hand, amorphous silica substrates have no preferential orientation and thereby impart none to the surfactant molecules. Noncontact atomic force imaging was used to image adsorbed surfactant layers on mica and graphite (155), revealing that micelles will adopt a cylinder or hemicylindrical configuration depending on the nature of the substrate (Figure 10). Spheres and hemispheres were also observed under different conditions (156). This micellar organization at the interface is largely unchanged by the presence of silicate precursors (18). The interfacial interactions affect the micellar organization in two ways: (*a*) on most surfaces, the micellar structures will align parallel to the plane of the interface ("in-plane confinement"); and (*b*) for strongly interacting substrates (e.g. graphite and mica), the micellar structures in each layer will be oriented along one or more preferred directions ["in-plane orientation" (18, 86; Figure 10)].

It is unlikely that epitaxial deposition can be used as an explanation of the mode of adsorption because the diameters of the individual micelles are much larger than the underlying unit cells. The interface may instead impose physical and/or energetic constraints on the first micellar layer, effectively confining it to the plane of the interface. Subsequent layers would then be influenced by the configuration of the first layer. Based on previous models, two types of interfacial interactions were hypothesized to explain in-plane confinement: (*a*) a Helfrich-type bending energetic effect (157) and/or (*b*) electrostatic or other surface-micelle interactions (86). The Helfrich bending-energy model predicts that micellar structures possess a spontaneous curvature in three dimensions. The presence of a surface restricts micellar motion, thereby creating an energetic incentive for in-plane confinement

of the structure. Electrostatic and other energetic interactions may complement the Helfrich bending-energy effect as well as affect in-plane orientation.

Air/Liquid Interfaces In contrast to studies on solid/liquid interfaces, studies of organization at the air/liquid interface are hampered by the soft structures that form at the air/liquid interface. Attempts to circumvent this limitation seek to extrapolate the solid/liquid interface to the more pliable air/liquid interface by treating the latter as a weakly interacting, hydrophobic surface (86). Furthermore, the structural evolution of mesoscopic silica films grown at the air/liquid interface has primarily been studied in dilute, acidic (pH < 2) systems (33, 93, 100, 107, 151, 158). This system offers the advantages that films can be easily grown, collected, and characterized. In addition, a complete body of literature describing the evolution and final structure of the films exists. Finally, the air/liquid interface is an intermediate energetic environment between strongly interacting solid substrates and bulk solution (in the limit of no surface interaction, particles are formed).

Extensive characterizations of mesoporous silicates formed under acidic conditions (91, 93, 95, 96, 100, 102, 105–107) indicate that the mesopores grow by continuously accreting silicate micelles from solution onto "liquid-crystalline" surfactant-silicate seeds [$\sim$50 nm in size (96)]. It is suggested that these seeds can organize into surface-confined, hexagonal domains that are oriented in parallel to the surface through the influence of a surfactant hemimicellar overstructure at the air/liquid interface (93, 99, 100). But this model may be incomplete (103, 109–111); other studies reveal an induction period preceding the onset of mesoscopic order (103, 109). Although there is an accumulation of material at the interface during the induction period, mesoscopic ordering within the developing film could not be detected, but a mesoscopic, hexagonally ordered structure that is parallel to the interface appears by the end of the induction period (110, 111). Evidence of an intermediate cubic-phase structure has also been observed (111). Considered together, these results may reveal a transition from an amorphous phase to an ordered phase that occurs at the mesoscopic level, but scattering data are heretofore insufficient to show how such a transition might occur.

A disordered-to-ordered transition in the solid phase at the air/liquid interface suggests that ordering within the film proceeds through a multistep process and not through direct growth of multiple mesoscopic crystals that are formed from solution (86). Conditions early in the process have a marked effect on the final film structure by influencing the size and alignment of the initial ordered domains, especially when those conditions influence the nucleation of ordered grains. This latter point has been demonstrated by using induced alignment through the application of electric fields (60), magnetic fields (115), and shear (159), respectively. In these reports, the orientation of the mesoscopic materials was set by the application of the respective fields.

Disorder-to-order transitions may be evidence of a unified mechanism for the growth of mesoporous silica across all morphologies (86). Work on mesopores that are formed under alkaline conditions (113) demonstrates that phase transitions

can occur within the liquid-crystalline surfactant-silicate mesophase. Also, liquid-crystalline seeds have been observed (114), which supports the hypothesis that disorder-to-order transitions in the condensed phase may be a general mechanism in the development of mesoscopic order (86).

Micropatterned Thin Films It has been shown that microfabrication is possible using self-assembled monolayers (160–162) or microcapillary infiltration (163–165). Both processes form functional ceramics by using microcontact printing (160, 163–165). The micromolding process is quite flexible and has been used for the patterning of oriented mesoporous films composed of silica (60, 67, 164, 166, 167), niobia, and titania (67). The resulting materials are hierarchically ordered over several length scales—10 nm to several micrometers—and structures can be "tuned" through the choice of polymers, pattern, and/or colloidal particles [when used as a templating agent (67)].

Microcontact printing can be used to impose a hierarchy of microscopic structures on thin solid films by combining the use of surfactant self-assembly for templating with micromolding (60, 163; Figure 11). As noted above, micromolding in turn can be enhanced through the application of a field, which can be used to orient the mesoporous channels within the micrometer-sized channels of the micromold (typically made of polydimethyl siloxane). Because microcontact printing is independent of the substrate-surfactant interaction, it permits the formation of oriented nanostructures on any (nonconducting) substrate. Although the mechanism of this alignment is not fully understood, the ability to do so opens the possibility of pattern formation on any substrate even in the absence of epitaxy. However, the relative effects of the applied field versus geometrical confinement on the orientation of surfactant micellar structures remains an open topic of research.

Disordered Structures as Monoliths Disordered structures avoid the formation of grain boundaries inherent in the use of crystalline materials. Because the randomized pore network permeates the structure, the pore volume is more accessible

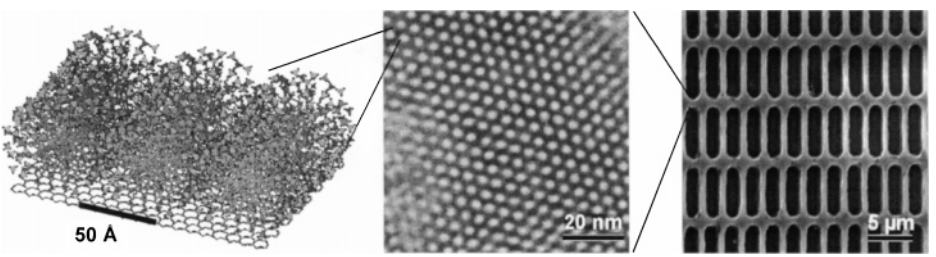

Figure 11 Liquid-crystal templating begins at the molecular scale through the interactions of the inorganic precursor with the surfactant structure [here shown as aligned tubules on a mica substrate (*left*)]. The tubules can be ordered into hexagonal array (*center*) and through the use of micromolding (*right*) formed into larger structures at the micrometer level.

and avoids disadvantages associated with oriented anisotropic structures. As such, these materials can be more readily applied to the synthesis of larger-scale structures in which pore accessibility is important to eventual application (such as in membranes and catalyst supports).

Silicates will nucleate and grow on the surface of a liquid-crystalline L_3 ("sponge") phase through the silicification of the surfaces of the randomly oriented pore structure (Figure 8). This process is used to form mesostructured monoliths and films with tunable pore dimensions from 10 to >100 nm (58, 59). The L_3 phase is a true liquid crystal, a thermodynamically stable phase in the system 1-hexadecylpyridinium chloride/hexanol/brine (168, 169). The phase consists of a three-dimensional random packing of a multiply connected and continuous membrane; the resulting pore network permeates the entire structure. Existing between the lamellar and reverse micellar phases, the L_3 phase can be regarded as a three-dimensional isotropic randomization of the cubic phase. The L_3 phase maintains bicontinuity in its bilayer structure, with negative Gaussian curvature and subdivision of the solvent phase into two equivalent volumes (for example, see 168).

As a bilayer structure, the primary pore volume in the L_3 silicate is filled with solvent, not surfactant, so that the void space is immediately available for infiltration without the need to remove the organic template. Also, the pore size is determined solely by the amount of solvent, with increasing solvent content increasing the characteristic pore diameter in the monolith—the "dilution effect" (168). When necessary, the surfactant can be removed through thermolysis or solvent or supercritical extraction, processes that may open a third continuous-pore network within the walls of the bilayer. These materials remain optically transparent owing to the large size of the primary pores, with measured surface areas within the range of 600–1400 m^2/g.

A disordered structure is also the result of polymerizing silicate anions that surround surfactant micelles in the presence of organic salts (119). The pore structure of the resulting material, KIT-1 (119), is a three-dimensional, disordered network of short wormlike channels with uniform pore diameters. The entire mesostructure exhibits high hydrothermal stability along with a highly branched pore structure. It is thought that the presence of the organic salt transforms an underlying hexagonal phase into a disordered phase, which is very similar in appearance to the L_3 phase. Taken together, the importance of a structure-directing agent in the formation of a mesophase is demonstrated by these two disordered materials. The cosurfactant hexanol used in the formation of the L_3 liquid crystal perturbs an underlying ordered phase (e.g. cubic) in a manner that appears similar to the effect of the organic salt on the underlying hexagonal phase.

A sol-gel process that achieves self-organization between surfactant and silicate through weak van der Waals-type interactions has been developed to synthesize mesoporous silica in the form of optically transparent films, fibers, and plates (122, 123). The synthesis process involves hydrolyzing the silica precursor and, simultaneously, partially condensing it in nonaqueous solutions containing sub-stoichiometric amounts of water, acid, and surfactants. The solvent is subsequently evaporated so that the surfactant-silicate organization occurs through a

weak enthalpy effect and avoids entropic effects caused by mixing. This synthesis is controllable and can be used to form mesoporous channels with uniform diameters either hexagonally packed in parallel to the surface or randomly oriented. The morphology depends on the reactant ratios and degree of the silicate prepolymerization. Optically transparent mesoporous silica plates can be fabricated without cracking in diameters up to centimeters in length and in thicknesses of $\leq$0.5 mm. These plates have uniform birefringence, resembling a single crystal structure (122, 123).

Other silicates with disordered pore structures exhibiting wormlike morphologies have been prepared through the hydrolysis of tetraethoxysilane in the presence of polyethylene oxide surfactants acting as the structure-directing agents (120, 121, 125, 126). This process differs from the L_3 phase described above in that it uses a nonionic surfactant as the template, which interacts with a neutral inorganic precursor via hydrogen bonding to form the mesostructures. The interaction occurs between the hydrophilic surfaces of flexible rod- or wormlike micelles and the silicon alkoxide to form the mesostructure (an example of an S^0I^0 mechanism) (125). The resulting channels also exhibit uniform diameters ranging from 2.0 to 5.8 nm, which can be varied by changing the size and structure of the surfactant molecules. Metal-substituted silica and pure alumina mesostructures have also been prepared by the hydrolysis of the corresponding alkoxides in the presence of the polyethylene oxide surfactants, suggesting a general application for nonionic templating in fabricating mesoporous oxides. More generally, these researchers have demonstrated that the S^0I^0 mechanism can be easily tailored through the use of structure-modifying agents (125).

CONCLUSION

Similar to the processes observed for biogenic composites, the architectures generated through self-assembly of surfactants or macromolecules can serve as templates to process ceramics with nanostructured patterns. The examples described in this review illustrate the potential of this general approach as an alternative processing methodology, especially in applications in which substrates cannot be exposed to high temperatures. The method is ideal for processing organic/inorganic nanocomposites. Removing the organic phase yields nanostructured ceramic "scaffoldings" or cellular solids that can in turn be used as the base for the fabrication of hierarchical ceramic-ceramic or ceramic-metal composites. The advent of block copolymer processing offers a new venue for the fabrication of large-scale structures, with which the potential of these materials may soon be realized.

ACKNOWLEDGMENTS

Our work was supported by the U.S. Army Research Office (grant DAAH04-95-1-0102) and the Materials Research Science and Engineering Center of the National Science Foundation (DMR-9809483).

LITERATURE CITED

1. McGehee MD, Gruner SM, Yao N, Chun CM, Navrotsky A, Aksay IA. 1994. *Proc. Annu. Meet. Microsc. Soc. Am., 52nd, New Orleans, LA*, ed. GW Bailey, AJ Garret–Reed, pp. 448–49. San Francisco, CA: San Francisco Press
2. Weissman JM, Sunkara HB, Tse AS, Asher SA. 1996. *Science* 274:959–60
3. Subramanian G, Manoharan VN, Thorne JD, Pine DJ. 1999. *Adv. Mater.* 11:1261–65
4. Adams M, Dogic Z, Keller SL, Fraden S. 1998. *Nature* 393:349–52
5. Burmeister F, Schafle C, Keilhofer B, Bechinger C, Boneberg J, Leiderer P. 1998. *Adv. Mater.* 10:495–97
6. Poulin P. 1999. *Curr. Opin. Colloid Interface Sci.* 4:66–71
7. Dinsmore AD, Crocker JC, Yodh AG. 1998. *Curr. Opin. Colloid Interface Sci.* 3:5–11
8. Ramsay JDF. 1996. *Curr. Opin. Colloid Interface Sci.* 1:208–13
9. Jiang P, Hwang KS, Mittleman DM, Bertone JF, Colvin VL. 1999. *J. Am. Chem. Soc.* 121:11630–37
10. Pan GS, Kesavamoorthy R, Asher SA. 1998. *J. Am. Chem. Soc.* 120:6525–30
11. Grier DG. 1998. *Mater. Res. Soc. Bull.* 23:21
12. Fendler JH. 1996. *Chem. Mater.* 8:1616–24
13. Kresge CT, Leonowicz ME, Roth WJ, Vartuli JC, Beck JS. 1992. *Nature* 359:710–12
14. Beck JS, Vartuli JC, Roth WJ, Leonowicz ME, Kresge CT, et al. 1992. *J. Am. Chem. Soc.* 114:10834–43
15. McGehee MD. 1994. *Self-assembling mesoscopic surfactant/silicate materials.* BS degree. Princeton Univ., Princeton, NJ. 64 pp.
16. Comm. Synthetic Hierarchical Struct., Nat. Res. Counc. 1994. *Hierarchical Structures in Biology as a Guide for New Materials Technology.* Washington, DC: Natl. Acad. Sci. Press
17. Sarikaya M, Aksay IA, eds. 1995. *Biomimetics: Design and Processing of Materials.* New York: Am. Inst. Phys. 352 pp.
18. Aksay IA, Trau M, Manne S, Honma I, Yao N, et al. 1996. *Science* 273:892–98
19. Aksay IA, Weiner S. 1998. *Curr. Opin. Solid State Mater. Sci.* 3:219–20
20. Aksay IA, Baer E, Sarikaya M, Tirrell DA, eds. 1992. *Hierarchically Structured Materials.* Pittsburgh, PA: Mater. Res. Soc. 255 pp.
21. Coombs N, Khushalani D, Oliver S, Ozin GA, Shen GC, et al. 1997. *J. Chem. Soc. Dalton Trans.* (21):3931–52
22. Alivisatos AP, Barbara PF, Castleman AW, Chang J, Dixon DA, et al. 1998. *Adv. Mater.* 10:1297–336
23. Goltner CG, Antonietti M. 1997. *Adv. Mater.* 9:431–36
24. Tomalia DA, Wang ZG, Tirrell M. 1999. *Curr. Opin. Colloid Interface Sci.* 4:3–5
25. Meier W. 1999. *Curr. Opin. Colloid Interface Sci.* 4:6–14
26. Mann S, Burkett SL, Davis SA, Fowler CE, Mendelson NH, et al. 1997. *Chem. Mater.* 9:2300–10
27. Raman NK, Anderson MT, Brinker CJ. 1996. *Chem. Mater.* 8:1682–701
28. Guizard CG, Julbe AC, Ayral A. 1999. *J. Mater. Chem.* 9:55–65
29. Ying JY, Mehnert CP, Wong MS. 1999. *Angew. Chem. Int. Ed. Engl.* 38:56–77
30. Safinya CR, Addadi L. 1996. *Curr. Opin. Solid State Mater. Sci.* 1:387–91
31. Addadi L, Safinya CR. 1997. *Curr. Opin. Solid State Mater. Sci.* 2:325–29
32. Thompson DW. 1992. *On Growth and*

Form: The Complete Revised Edition. New York: Dover. 1095 pp.
33. Xu GF, Yao N, Aksay IA, Groves JT. 1998. *J. Am. Chem. Soc.* 120:11977–85
34. Mann S. 1997. *J. Chem. Soc. Dalton Trans.* (21):3953–61
35. Baer E, Hiltner A, Morgan RJ. 1992. *Phys. Today* 45:60–67
36. Baer E. 1987. *Science* 235:1015–22
37. Aksay IA. 1996. In *Frontier Nanostructured Ceramics*, pp. 35–41. Fukuoka, Jpn: Tohwa Univ.
38. Mann S, Ozin GA. 1996. *Nature* 382:313–18
39. Lowenstam HA, Weiner S. 1989. *On Biomineralization.* Oxford, UK: Oxford Univ. Press
40. Heywood BR, Mann S. 1992. *Langmuir* 8:1492–98
41. Mann S. 1993. *J. Chem. Soc. Dalton Trans.* (1):1–9
42. Siegel RW. 1993. *Phys. Today* 46:64–68
43. Lakes R. 1993. *Nature* 361:511–15
44. Lurie KA, Cherkaev AV. 1984. *Proc. R. Soc. Edinburgh A* 99:71–87
45. Sarikaya M, Aksay IA. 1992. *Structure, Cellular Synthesis and Assembly of Biopolymers*, ed. ST Case, pp. 1–25. New York: Springer
46. Zaremba CM, Belcher AM, Fritz M, Li YL, Mann S, et al. 1996. *Chem. Mater.* 8:679–90
47. Schäffer TE, Ionescu Zanetti C, Proksch R, Fritz M, Walters DA, et al. 1997. *Chem. Mater.* 9:1731–40
48. Fritz M, Morse DE. 1998. *Curr. Opin. Colloid Interface Sci.* 3:55–62
49. Halverson DC, Pyzik AJ, Aksay IA. 1986. *US Patent No. 4605440*
50. Pyzik AJ, Aksay IA. 1987. *US Patent No. 4702770*
51. Aksay IA, Yasrebi M, Milius DL, Kim G-H, Sarikaya M. 1994. *US Patent No. 5308422*
52. Mueller CD, Nazarenko S, Ebeling T, Schuman TL, Hiltner A, Baer E. 1997. *Polym. Eng. Sci.* 37:355–62
53. Halverson DC, Pyzik AJ, Aksay IA, Snowden WE. 1989. *J. Am. Ceram. Soc.* 72:775–80
54. Yasrebi M, Kim GH, Gunnison KE, Milius DL, Sarikaya M, Aksay IA. 1990. Better ceramics through chemistry. *Proc. Mater. Res. Soc. Symp. 4th*, ed. BJJ Zelinski, CJ Brinker, DE Clark, DR Ulrich, pp. 625–35. Pittsburgh, PA: Mater. Res. Soc.
55. Kim GH, Sarikaya M, Milius DL, Aksay IA. 1989. *Proc. Annu. Meet. Electron Microsc. Soc. Am., 47th*, ed. GW Bailey, pp. 562–63. San Francisco, CA: San Francisco Press
56. Currey JD, Biggs WD, Wainwright SA. 1982. *Mechanical Design in Organisms.* Princeton, NJ: Princeton Univ. Press. 436 pp.
57. Lahiri J, Xu G, Dabbs DM, Yao N, Aksay IA, Groves JT. 1997. *J. Am. Chem. Soc.* 119:5449–50
58. McGrath KM, Dabbs DM, Yao N, Aksay IA, Gruner S. 1997. *Science* 277:552–56
59. McGrath KM, Dabbs DM, Yao N, Edler KJ, Aksay IA, Gruner SM. 2000. *Langmuir* 16:398–406
60. Trau M, Yao N, Kim E, Xia Y, Whitesides GM, Aksay IA. 1997. *Nature* 390:674–76
61. Trau M, Sankaran S, Saville DA, Aksay IA. 1995. *Nature* 374:437–39
62. Trau M, Sankaran S, Saville DA, Aksay IA. 1995. *Langmuir* 11:4665–72
63. Trau M, Saville DA, Aksay IA. 1996. *Science* 272:706–9
64. Trau M, Saville DA, Aksay IA. 1997. *Langmuir* 13:6375–81
65. Gau H, Herminghaus S, Lenz P, Lipowsky R. 1999. *Science* 283:46–49
66. Gallardo BS, Gupta VK, Eagerton FD, Jong LI, Craig VS, et al. 1999. *Science* 283:57–60
67. Yang P, Deng T, Zhao D, Feng P, Pine D, et al. 1998. *Science* 282:2244–46
68. Zhou W, Thomas JM, Shephard DS, Johnson BFG, Ozkaya D, et al. 1998. *Science* 280:705–8

69. Holland BT, Blanford CF, Stein A. 1998. *Science* 281:538–40
70. Park M, Harrison C, Chaikin PM, Register RA, Adamson DH. 1997. *Science* 276: 1401–4
71. Stupp SI, Braun PV. 1997. *Science* 277: 1242–48
72. Muthukumar M, Ober CK, Thomas EL. 1997. *Science* 277:1225–32
73. Schacht S, Huo Q, Voigt-Martin IG, Stucky GD, Schuth F. 1996. *Science* 273:768–71
74. Aizenberg J, Black AJ, Whitesides GM. 1999. *Nature* 398:495–98
75. Mann S, Webb J, Williams RJP, eds. 1989. *Biomineralization: Chemical and Biochemical Perspectives*. New York: VCH Publ. 541 pp.
76. Mann S. 1993. *Nature* 365:499–505
77. Campbell AA. 1999. *Curr. Opin. Colloid Interface Sci.* 4:40–45
78. Liu J, Kim A, Wang LQ, Palmer BJ, Chen YL, et al. 1996. *Adv. Colloid Interface Sci.* 69:131–80
79. Yanagisawa T, Shimizu T, Kuroda K, Kato C. 1990. *Bull. Chem. Soc. Jpn.* 63:988–92
80. Chiola V, Ritsko JE, Vanderpool CD. 1971. *US Patent No. 3556725*
81. Di Renzo F, Cambon H, Dutarte R. 1997. *Microporous Mater.* 10:283–86
82. Schuth F. 1998. *Curr. Opin. Colloid Interface Sci.* 3:174–80
83. Vartuli JC, Schmitt KD, Kresge CT, Roth WJ, Leonowicz ME, et al. 1994. *Chem. Mater.* 6:2317–26
84. Hue QS, Margolese DI, Ciesla U, Feng P, Gier TE, et al. 1994. *Nature* 368:317–21
85. Monnier A, Schüth F, Huo Q, Kumar D, Margolese D, et al. 1993. *Science* 261: 1299–303
86. Yao N, Ku AY, Nakagawa H, Lee T, Saville DA, Aksay IA. 2000. *Chem. Mater.* 12:1536–548
87. Sun T, Ying JY. 1997. *Nature* 389:704–6
88. Wong MS, Ying JY. 1998. *Chem. Mater.* 10:2067–77
89. Huo Q, Margolese DI, Ciesla U, Demuth DG, Feng P, et al. 1994. *Chem. Mater.* 6:1176–91
90. Huo Q, Margolese DI, Stucky GD. 1996. *Chem. Mater.* 8:1147–60
91. Huo Q, Zhao D, Feng J, Weston K, Buratto SK, et al. 1997. *Adv. Mater.* 9:974–78
92. Zhao DY, Feng JL, Huo QS, Melosh N, Fredrickson GH, et al. 1998. *Science* 279: 548–52
93. Yang H, Ozin GA, Kresge CT. 1998. *Adv. Mater.* 10:883–87
94. Yang H, Coombs N, Ozin GA. 1997. *Nature* 386:692–95
95. Yang H, Vovk G, Coombs N, Sokolov I, Ozin GA. 1998. *J. Mater. Chem.* 8:743–50
96. Yang H, Coombs N, Sokolov I, Kresge CT, Ozin GA. 1999. *Adv. Mater.* 11:52–55
97. Schmidt-Winkel P, Yang P, Margolese DI, Chmelka BF, Stucky GD. 1999. *Adv. Mater.* 11:303–7
98. Lu Y, Fan H, Stump A, Ward TL, Rieker T, Brinker CJ. 1999. *Nature* 398:223–26
99. Yang H, Coombs N, Sokolov I, Ozin GA. 1996. *Nature* 381:589–92
100. Yang H, Coombs N, Dag O, Sokolov I, Ozin GA. 1997. *J. Mater. Chem.* 7:1755–61
101. Yao N, Trau M, Manne S, Nakagawa N, Lee T, Honma I, Aksay IA. 1997. In *Proc. Microscopy and Microanalysis*, ed. GW Bailey, RVW Dimlich, KB Alexander, JJ McCarthy, TP Pretlow, pp. 395–96. New York, NY: Springer-Verlag
102. Yang H, Coombs N, Ozin GA. 1997. *Adv. Mater.* 9:811–14
103. Brown AS, Holt SA, Dam T, Trau M, White JW. 1997. *Langmuir* 13:6363–65
104. Lu Y, Ganguli R, Drewien CA, Anderson MT, Brinker CJ, et al. 1997. *Nature* 389:364–68
105. Yang H, Kuperman A, Coombs N, MamicheAfara S, Ozin GA. 1996. *Nature* 379:703–5

106. Yang H, Coombs N, Sokolov I, Ozin GA. 1997. *J. Mater. Chem.* 7:1285–90
107. Yang H, Coombs N, Ozin GA. 1998. *J. Mater. Chem.* 8:1205–11
108. Roser SJ, Patle HM, Lovell MR, Muir JE, Mann S. 1998. *Chem. Commun.* 7:829–30
109. Brown AS, Holt SA, Reynolds PA, Penfold J, White JW. 1998. *Langmuir* 14:5532–38
110. Holt SA, Foran GJ, White JW. 1999. *Langmuir* 15:2540–42
111. Ruggles JL, Holt SA, Reynolds PA, Brown AS, Creagh DC, White JW. 1999. *Phys. Chem. Chem. Phys.* 1:323–28
112. Feng J, Huo Q, Petroff PM, Stucky GD. 1997. *Appl. Phys. Lett.* 71:1887–89
113. Firouzi A, Atef F, Oertli AG, Stucky GD, Chmelka BF. 1997. *J. Am. Chem. Soc.* 119:3596–610
114. Regev O. 1996. *Langmuir* 12:4940–44
115. Tolbert SH, Firouzi A, Stucky GD, Chmelka BF. 1997. *Science* 278:264–68
116. Anderson MT, Martin JE, Odinek JG, Newcomer PP. 1998. *Chem. Mater.* 10: 311–21
117. Hyde ST. 1996. *Curr. Opin. Solid State Mater. Sci.* 1:653–62
118. Alfredsson V, Anderson MW, Ohsuna T, Terasaki O, Jacob M, Bojrup M. 1997. *Chem. Mater.* 9:2066–70
119. Ryoo R, Kim JM, Ko CH, Shin CH. 1996. *J. Phys. Chem.* 100:17718–21
120. Tanev PT, Pinnavaia TJ. 1996. *Chem. Mater.* 8:2068–79
121. Pauly TR, Liu Y, Pinnavaia TJ, Billinge SJL, Rieker TP. 1999. *J. Am. Chem. Soc.* 121:8835–42
122. Ko CH, Kim JM, Ryoo R. 1998. *Micropor. Mesopor. Mater.* 21:235–43
123. Ryoo R, Ko CH, Cho SJ, Kim JM. 1997. *J. Phys. Chem. B* 101:10610–13
124. Anderson MT, Martin JE, Odinek JG, Newcomer PP. 1998. *Chem. Mater.* 10:1490–500
125. Zhang WZ, Pauly TR, Pinnavaia TJ. 1997. *Chem. Mater.* 9:2491–98
126. Bagshaw SA, Prouzet E, Pinnavaia TJ. 1995. *Science* 269:1242–44
127. Li WZ, Xie SS, Qian LX, Chang BH, Zou BS, et al. 1996. *Science* 274:1701–3
128. Sakai H, Baba R, Hashimoto K, Fujishima A, Heller A. 1995. *J. Phys. Chem.* 99:11896–900
129. Ye C, Tamagawa T, Schiller P, Polla DL. 1992. *Sens. Act. A* 35:77–83
130. Jenekhe SA, Chen XL. 1999. *Science* 283:372–75
131. Chan VZH, Hoffman J, Lee VY, Iatrou H, Avgeropoulos A, et al. 1999. *Science* 286:1716–19
132. Templin M, Franck A, Du Chesne A, Leist H, Zhang Y, et al. 1997. *Science* 278:1795–98
133. Ulrich R, Du Chesne A, Templin M, Wiesner U. 1999. *Adv. Mater.* 11:141–46
134. Matsen MW, Schick M. 1996. *Curr. Opin. Colloid Interface Sci.* 1:329–36
135. Matsen MW. 1998. *Curr. Opin. Colloid Interface Sci.* 3:40–47
136. Goldacker H, Tabetz V, Stadler R, Erukhimovich I, Leibler L. 1999. *Nature* 398:137–39
137. Cha JN, Stucky GD, Morse DE, Deming TJ. 2000. *Nature* 403:289–92
138. Cummins CC, Beachy MD, Schrock RR, Vale MG, Sankaran V, Cohen RE. 1991. *Chem. Mater.* 3:1153–63
139. Yue J, Cohen RE. 1994. *Supramol. Sci.* 1:117–22
140. Harrison CK, Adamson DH, Park M, Chaikin PM, Register RA. 1997. *Abstr. Pap. Am. Chem. Soc.* 214:116
141. Morkved TL, Lu M, Urbas AM, Ehrichs EE, Jaeger HM, et al. 1996. *Science* 273:931–33
142. Anastasiadis SH, Russell TP, Satija SK, Majkrzak CF. 1989. *Phys. Rev. Lett.* 2:1852–55
143. Wakino K, Mirai K, Tamura H. 1984. *J. Am. Ceram. Soc.* 67:278–81
144. Maurice AK, Buchanan RC. 1987. *Ferroelectrics* 74:61–75

145. Begg BD, Vance ER, Nowotny J. 1994. *J. Am. Ceram. Soc.* 77:3186–92
146. Slamovich EB, Aksay IA. 1994. *MRS Symp. Proc* 346:63–8
147. Slamovich EB, Aksay IA. 1996. *J. Am. Ceram. Soc.* 79:239–47
148. Lee T, Yao N, Aksay IA. 1997. *Langmuir* 13:3866–70
149. Luther EP, Chun CM, Lee T, Aksay IA. 1998. In *Advances in Dielectric Ceramic Materials*, ed. KM Nair, AS Bhalla, pp. 189–94. Westerville, OH: Am. Ceram. Soc.
150. Zhao D, Yang P, Huo Q, Chmelka BF, Stucky GD. 1998. *Curr. Opin. Solid State Mater. Sci.* 3:111–21
151. Zhao D, Yang P, Melosh N, Feng J, Chmelka BF, Stucky GD. 1998. *Adv. Mater.* 10:1380–85
152. Corma A, Kan QB, Navarro MT, Perez-Pariente J, Rey F. 1997. *Chem. Mater.* 9:2123–26
153. Cyr DM, Venkataraman B, Flynn GW. 1996. *Chem. Mater.* 8:1600–15
154. Manne S, Cleveland JP, Gaub HE, Stucky GD, Hansma PK. 1994. *Langmuir* 10:4409–13
155. Manne S, Gaub HE. 1995. *Science* 270:1480–82
156. Patrick HN, Warr GG, Manne S, Aksay IA. 1999. *Langmuir* 15:1685–92
157. Helfrich W. 1973. *Z. Naturforsch. Teil C* 28:693
158. Tolbert SH, Schaffer TE, Feng JL, Hansma PK, Stucky GD. 1997. *Chem. Mater.* 9:1962–67
159. Hillhouse HW, van Egmond JW, Tsapatsis M. 1999. *Langmuir* 15:4544–50
160. Kumar A, Biebuyck HA, Whitesides GM. 1994. *Langmuir* 10:1498–511
161. Bunker BC, Rieke PC, Tarasevich BJ, Campbell AA, Fryxell GE, et al. 1994. *Science* 264:48–55
162. Rieke PC, Tarasevich BJ, Wood LL, Engelhard MH, Baer DR, Fryxell GE. 1994. *Langmuir* 10:619–22
163. Kim E, Xia YN, Whitesides GM. 1995. *Nature* 376:581–84
164. Zhao XM, Xia YN, Whitesides GM. 1997. *J. Mater. Chem.* 7:1069–74
165. Xia YN, Whitesides GM. 1998. *Annu. Rev. Mater. Sci.* 28:153–84
166. Miyata H, Kuroda K. 2000. *Chem. Mater.* 12:49–54
167. Miyata H, Kuroda K. 1999. *J. Am. Chem. Soc.* 121:7618–24
168. Skouri M, Marignan J, Appell J, Porte G. 1991. *J. Phys. II Fr.* 1:1121–32
169. McGrath KM. 1997. *Langmuir* 13:1987–95
170. Weiner S, Wagner HD. 1998. *Annu. Rev. Mater. Sci.* 28:271–98

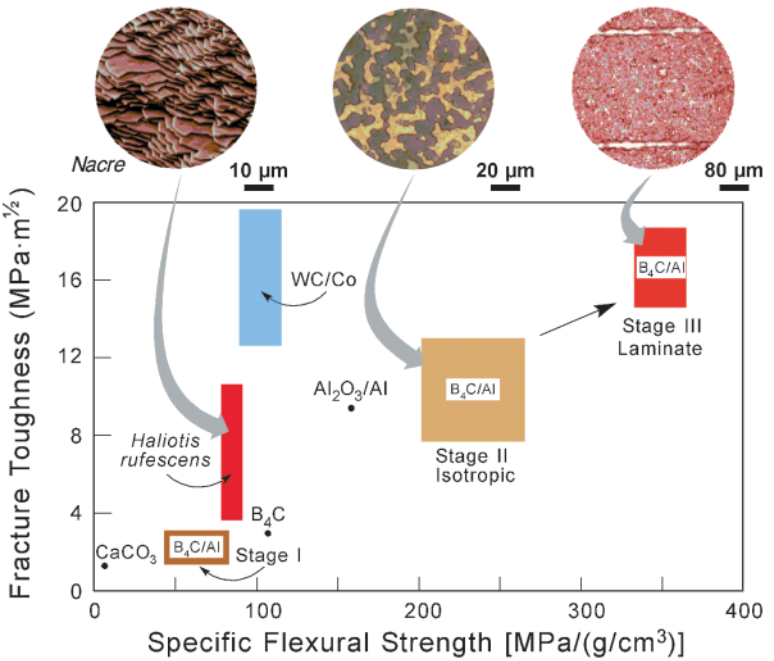

Figure 5 Significant improvements are achieved in the mechanical properties of ceramic-based composites if biogenic material designs are copied. Boron carbide/aluminum composites increased fourfold in toughness and strength as processing moved from infiltrated powder compacts (*Stage I*) through isostatic pressure infiltration (*Stage II*) to simple micrometer=C-scale laminates (*Stage III*). Although laminated, graded B_4C/Al composites (*upper right*) resemble the structure of seashell (*upper left*), the difference in scale is a palpable indication of the potential benefits if the scale of processing can be further reduced.

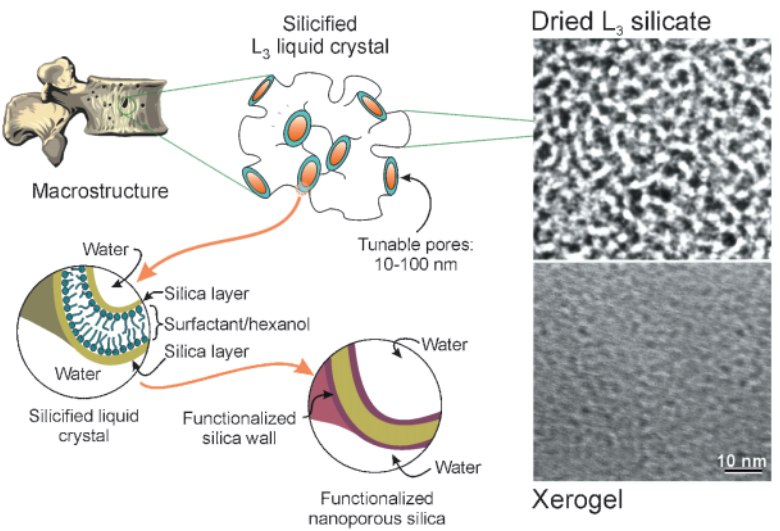

Figure 8 The *L3* liquid crystal can be used as a template for the formation of a mesostructured material. (*Left*) Pore dimensions are simply "tuned" by controlling the amount of solvent in the system (the "dilution rule") and the resulting mesostructure permeates the solution volume. The organic layer does not obstruct the pore volume, permitting immediate access to the pore network, but the organics can be removed through supercritical extraction. Functionalization of the silicate walls can be achieved through reinfiltration of the mesopore with appropriate functionalizing agents. The uniformity of the *L3* structure is evident in the transmission electron micrograph of an *L3* silicate (*upper right*) as compared to that of a comparable silica xerogel (*lower right*).

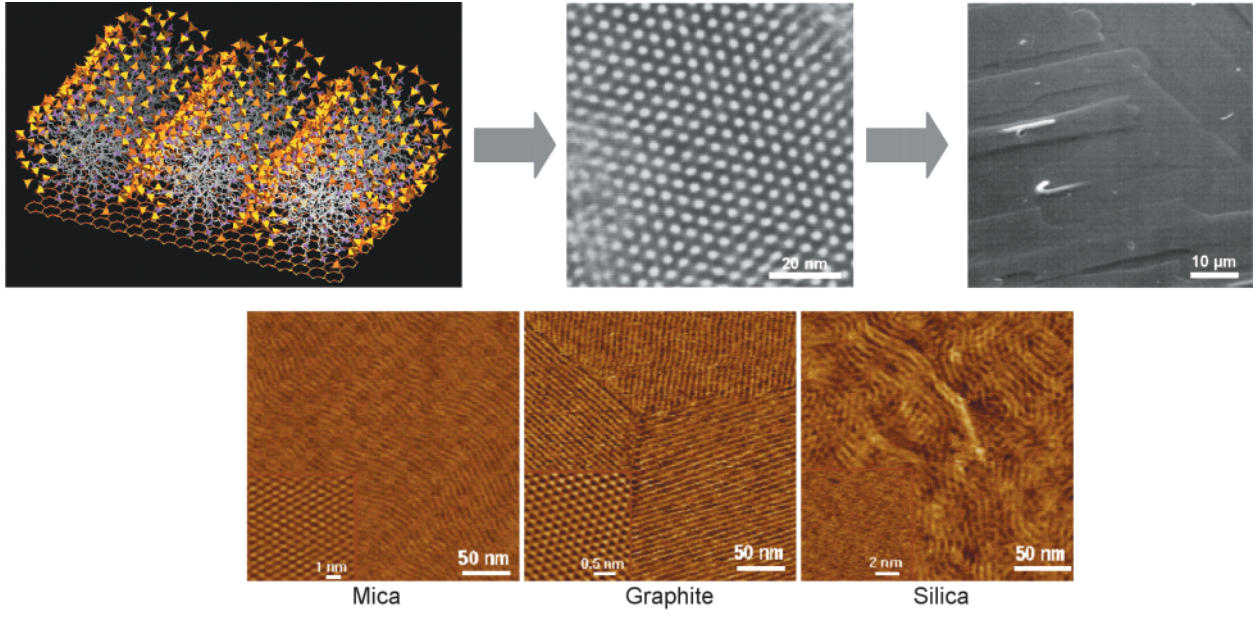

Figure 10 Development of mesostructured organic materials through liquid crystal templating. The process begins with the ordering of the liquid-crystalline phase (*top left*) which can be controlled by the crystal structure of the substrate (*bottom*). Aligned mesostructures (*top center*) form through orientation of subsequent layers by the previous layers, and this process can be used to create nanostructured thin films (*top right*).